Hepatic Segments and Vasculature: Projecting CT Anatomy onto Angiograms[1]

Toshihiro Furuta, MD, Eriko Maeda, MD, Hiroyuki Akai, MD,
Shouhei Hanaoka, MD, Naoki Yoshioka, MD, Masaaki Akahane, MD,
Takeyuki Watadani, MD, Kuni Ohtomo, MD

[1]From the Department of Radiology, University of Tokyo Hospital, 7-3-1, Hongo, Bunkyo-ku, Tokyo 113-8655, Japan. Received March 25, 2009; revision requested May 1 and received June 14; accepted July 2. Authors have no financial relationships to disclose. Address correspondence to T.F. (e-mail: tfuruta-tky@umin.ac.jp

Abbreviations: HCC = hepatocellular carcinoma, TACE/TAE = transarterial chemoembolization/transarterial embolization.

Arteries:
CHA = common hepatic artery
LGA = left gastric artery
LHA = left hepatic artery
PHA = proper hepatic artery
RHA = right hepatic artery
SMA = superior mesenteric artery
SpA = splenic artery

Abstract

Hepatic transarterial interventional therapies such as chemoembolization and radiation embolization are important treatment options for hepatocellular carcinoma. Understanding the anatomy of individual arterial branches and hepatic segments is critical for selecting the correct embolization technique for treatment and to avoid complications. The authors describe the morphologic characteristics of hepatic arterial branches (and their mimickers) and hepatic segments on conventional angiograms. These vessels and segments include the celiac artery, the common and proper hepatic arteries, the left and right hepatic arteries and branches, the caudate lobe, and the portal vein and branches. Mimickers of hepatic arteries include the cystic, accessory left gastric, and right gastric arteries, as well as branches of the left gastric artery that resemble segmental branches of the replaced left hepatic artery. The authors describe how each segmental branch of the hepatic artery and the area it supplies correlates at computed tomography (CT) and angiography. Finally, the authors demonstrate how the vascular anatomy changes with the respiratory cycle by creating a virtual movie from calculations with dynamic CT data, in which the arterial and venous phases are acquired at end expiration and inspiration, respectively. Each segmental branch of the hepatic artery has morphologic characteristics that help distinguish it from mimickers. The location of each hepatic segment can be estimated if the artery supplying the segment can be correctly identified on angiograms. Notably, morphologic differences in the hepatic artery system caused by respiration should be recognized.

Supplemental material available at

http://radiographics.rsna.org/lookup/suppl/doi:10.1148/rg.e37/-/DC1

TEACHING POINTS
See last page

Introduction

Hepatocellular carcinoma (HCC) is a common primary malignancy of the liver that generates 500 000 to 1 000 000 new patients worldwide annually and causes more than 650 000 deaths per year (1–3). The frequency of HCC is higher in regions such as East Asia and sub-Saharan Africa, but the incidence is increasing in Europe and in the United States (4,5). Most HCC arises in patients with cirrhosis that is often due to viral or alcoholic causes (1–5).

Transarterial chemoembolization or transarterial embolization (TACE/TAE) is an important treatment option for HCC because HCC replaces the dual supply provided by the arterial and portal blood flows to normal hepatic parenchyma with an arterial blood supply alone (6–8). A mixture of embolic agents (eg, gelatin sponge particles, polyvinyl alcohol particles, and iodized oil) with or without chemotherapeutic agents such as doxorubicin is delivered via a catheter during TACE/TAE.

Selective intraarterial radiation therapy, such as with yttrium 90 (^{90}Y) radioactive microbead embolization, is also effective for nonresectable liver tumors, including HCC. This therapy potentially confers a survival benefit with a low-toxicity profile (3,9).

The tip of the catheter can be positioned in the proper hepatic artery (PHA), right hepatic artery (RHA), or left hepatic artery (LHA) or in the segmental branches of the hepatic artery, depending on the location or distribution of the lesion to be treated. Selective catheterization with a microcatheter is desirable to preserve liver function and reduce side effects, especially when multiple lesions arise from a cirrhotic background.

Radiologists should understand the anatomy of the hepatic vasculature and confirm on conventional angiograms the location of an artery or lesion seen at CT. Embolization of the wrong branch due to lack of a correlated roadmap and lack of familiarity with variants of normal anatomy of liver vasculature can result in inadequate deposition of chemotherapeutic agents in the intended lesion or their unintended distribution. Furthermore, awareness of "mimickers" of segmental branches of the hepatic artery might prevent slow healing and complications such as ulceration of the cystic or gastric wall resulting from arterial embolization in these areas.

We describe the morphologic characteristics of each hepatic arterial branch and mimickers at angiography. We also describe how each segmental branch of the hepatic artery and the area it supplies correlate between CT and angiography. Finally, we show how the vascular anatomy changes with the respiratory cycle.

Historical Aspects of Liver Segmentation

The liver has been segmented in many ways since Hjortsjö established in 1951 the concept that biliary duct branching follows a segmental pattern (10). Healey and Schroy divided the liver into five segments by using secondary biliary duct and hepatic artery branching (11). Couinaud suggested that the liver should be divided into eight segments based on third-order portal vein distribution (12). Goldsmith and Woodburne divided the liver into four segments based on second-order portal branches (13). Bismuth then amalgamated the Couinaud and Goldsmith and Woodburne systems (14). Among these segmentations, naming of parts of the liver varied considerably: for example, lobes, divisions, sectors, segments, and subsegments. Sometimes the same terms had different meanings depending on the author. Thus, the Federative Committee on Anatomical Terminology published *Terminologia Anatomica* in 1998 to prevent confusion and unify the anatomic terminology (15). The most popular classifications of hepatic segments are compared in Figure 1.

Teaching Point

	Healey and Schroy (1953)		Couinaud (1957)		Goldsmith and Woodburne (1957)		Bismuth (1982)		FCAT (1998)	
	Segment	Subsegment	Sector	Segment	Segment	Subsegment	Sector	Segment	Sector	Segment
Dorsal	Caudate	Right / Left	Caudate lobe		Caudate lobe		Caudate lobe		Caudate lobe	
Left	Lateral	Superior	Lateral		Lateral	Superior	Posterior		Lateral	
		Inferior	Para-median			Inferior	Anterior			
	Medial	Superior			Medial	Superior			Medial	
		Inferior				Inferior				
Right	Anterior	Inferior	Para-median		Anterior	Inferior	Antero-medial		Medial	
		Superior				Superior				
	Posterior	Inferior	Lateral		Posterior	Inferior	Postero-lateral		Lateral	
		Superior				Superior				

Figure 1. The five most popular classifications of hepatic segments.

In this article, we basically follow the Couinaud system, which divides the liver into a total of eight subsegments according to portal anatomy.

Configurations of the Liver in Health and Cirrhosis

Patients undergoing TACE/TAE for HCC often have a background of cirrhosis similar to that in the cases presented here. S4 and the right lobe tend to become atrophic, while S2 and S3 become hypertrophic in cirrhosis (16). When applying our results to a healthy liver, deformities caused by cirrhosis must be corrected.

Morphologic Characteristics of Branches of the Hepatic Artery
Celiac Artery, Common Hepatic Artery (CHA), and PHA

The celiac artery emerges from the aorta at the level of the superior border of the pancreatic body (at about T12) (17–19). The celiac trunk branches into the following major branches of the celiac artery: CHA, left gastric artery (LGA), and splenic artery (SpA) (Fig 2). Although the celiac trunk divides into these three branches, branching patterns can vary considerably: for example, the hepatomesenteric type, which indicates CHA branching from the superior mesenteric artery (SMA); direct branching of the CHA, LGA, or SpA from the aorta; and replaced LHA and RHA (17–22). The CHA courses to the right along the superior ridge of the pancreas and then branches at the lower end of the epiploic foramen into the gastroduodenal artery and PHA. The PHA courses right and upward along the anterior border of the epiploic foramen and divides into the LHA and RHA at the hilum (17,21).
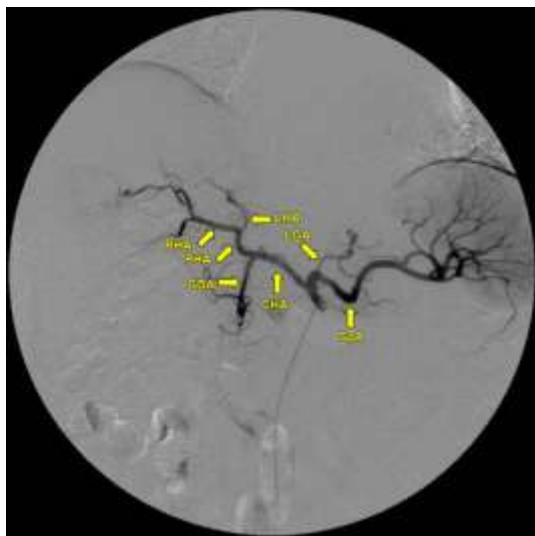
Figure 2. Arteriography of the three main branches of the celiac artery: the CHA, LGA, and SpA. The CHA divides into the PHA and gastroduodenal artery. The PHA divides into the LHA and RHA.
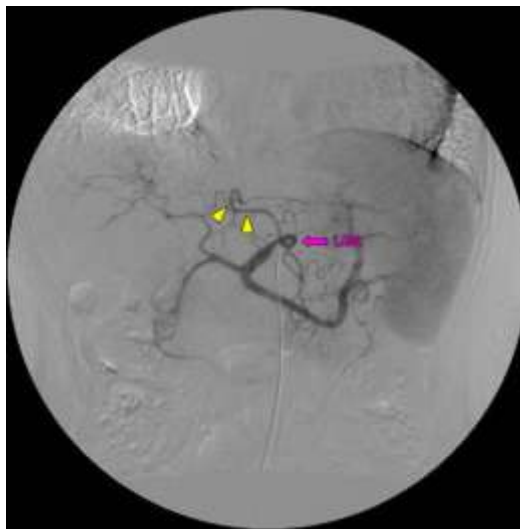
LHA and Branches

The LHA usually arises from the PHA, but when replaced it most commonly arises from the LGA (Fig 3) (17,19–24). Accessory LHAs arising from the LGA, celiac trunk or aorta must be considered (23,24). The LHA runs from the hepatic hilum to the umbilical portion of the left portal vein and usually to its right, coursing upward and leftward (Fig 4). At the posterior (dorsal) part of the umbilical portion of the left portal vein, the LHA overrides the portal vein to form the arch of the LHA. This arch is characteristic of the LHA and is helpful in distinguishing it from mimickers (25). After the arch, the LHA divides into the A2 and A3 branches (Fig 5). A2 branches from the distal end of the arch and courses straight to the left corner of the liver. A2 is usually situated superior to A3, which runs ventrally (caudally on the frontal view) along the left side of the umbilical portion, and then to the left.
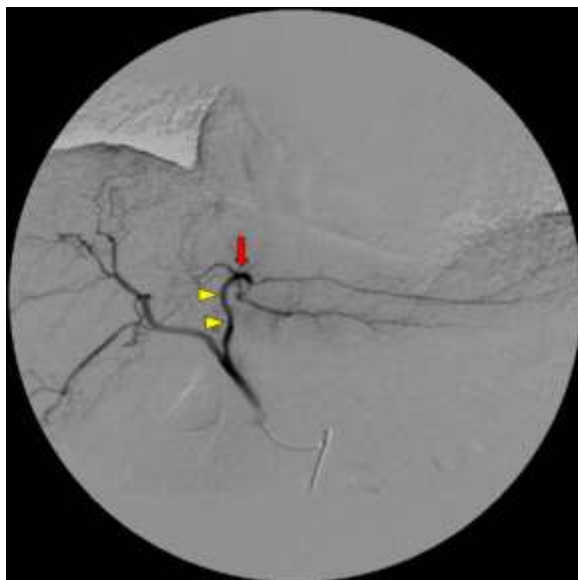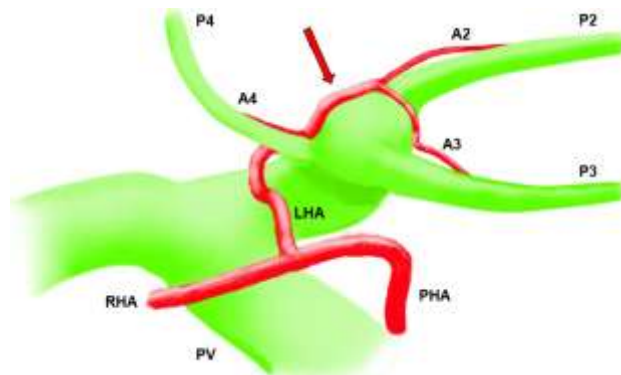
<div style="float:left">Teaching Point</div>

3a.

3b.

Figure 3. Celiac arteriography of **(a)** a conventional LHA (arrowheads) branching from the PHA and **(b)** a replaced LHA (arrowheads) branching from the LGA.

4a.   **4b.**

Figure 4. (a) PHA arteriography shows characteristic arch (arrow) of the LHA (arrowheads).
(b) Schematic of relationships between the LHA and portal vein (*PV*) in the umbilical portion.
The LHA forms an arch when it overrides the portal vein (arrow). *P2* = left posterior portal
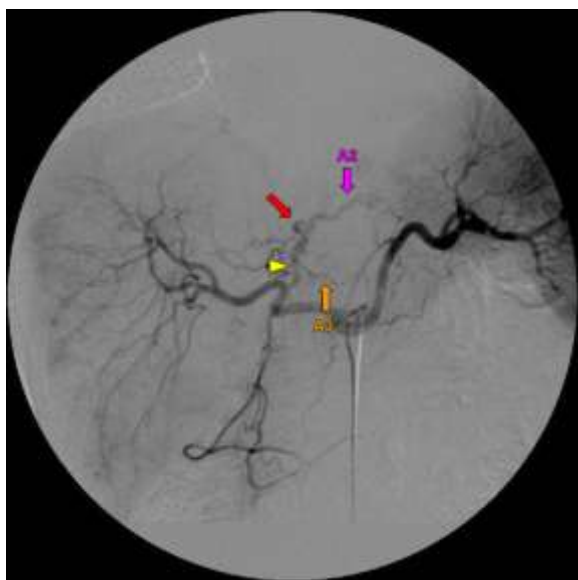branch, *P3* = left anterior portal branch, *P4* = left medial portal branch.

Figure 5. Celiac arteriography shows A2 and A3 branching from LHA (arrowhead) after the arch
(arrow).

The A4 branch has two main branching patterns (Fig 6). The conventional A4 of LHA
origin branches to the right from the proximal part of the umbilical portion. The A4 branch of
PHA origin, also called the middle hepatic artery, is determined when the trifurcating branch of
the PHA, other than the LHA or RHA, supplies S4 (17,19–21). A4 of both origins can coexist
(17,21)
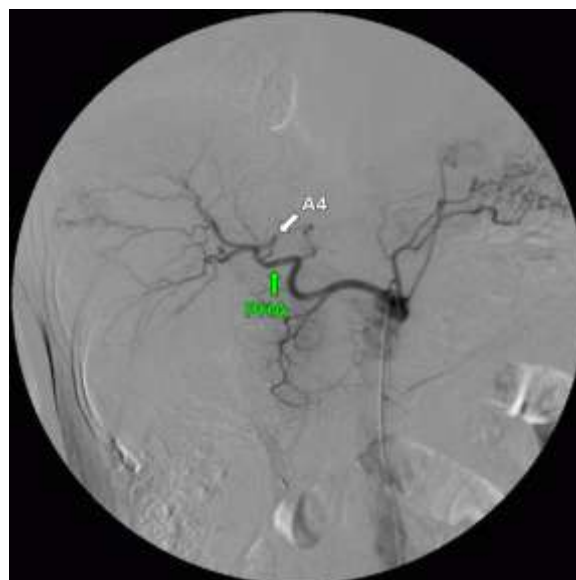
6a.   **6b.**

Figure 6. Celiac arteriography shows **(a)** conventional A4 branching from the LHA (arrowheads) and **(b)** A4 branching from the PHA.

RHA and Branches

The RHA usually arises from the PHA, and from the SMA when replaced (Fig 7) (17,19–24). Accessory RHAs arising from the SMA, the celiac trunk, or the aorta must be considered (23,24). The RHA divides into anterior and posterior branches that are characterized by a straight right upward course and by a meandering proximal portion, respectively (Fig 8) (26,27). Following the course of the arteries from the peripheral to the proximal portion is often helpful in discriminating these branches.
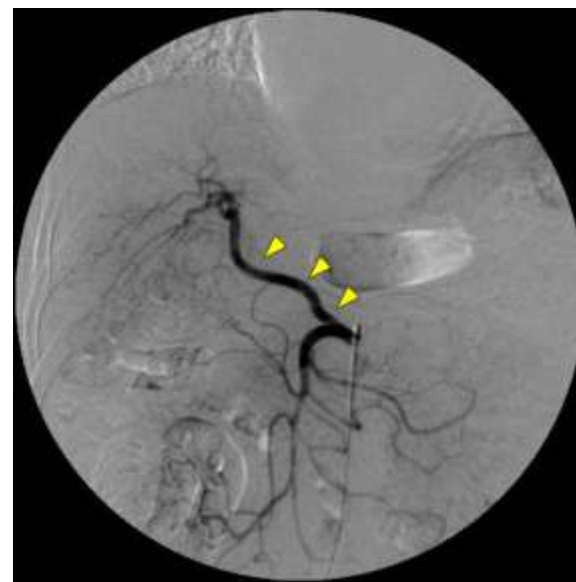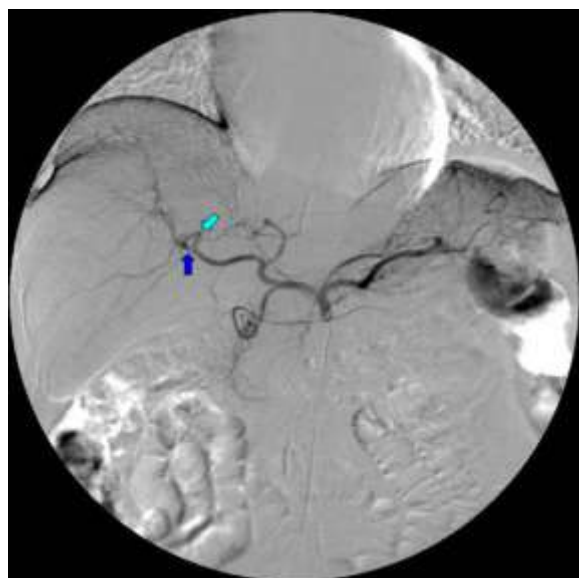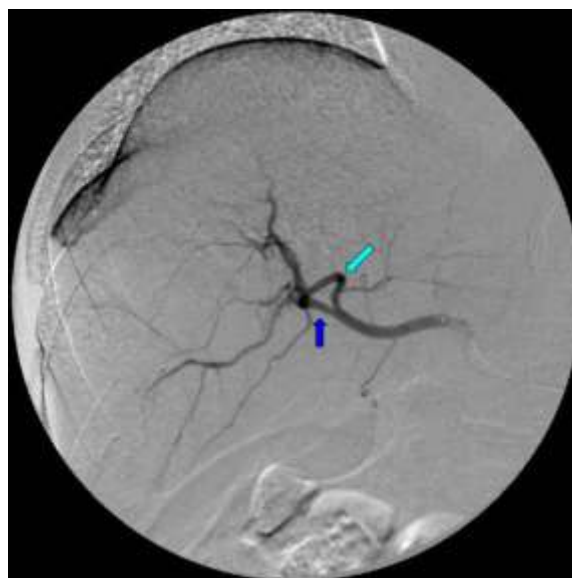

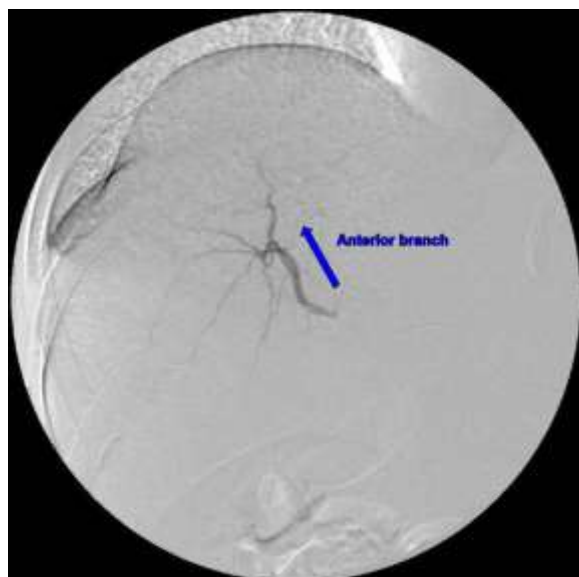**7a.**   **7b.**

Figure 7. (a) Celiac arteriography of conventional RHA (arrowheads) branching from the PHA. **(b)** SMA arteriography of replaced RHA (arrowheads) branching from the SMA.
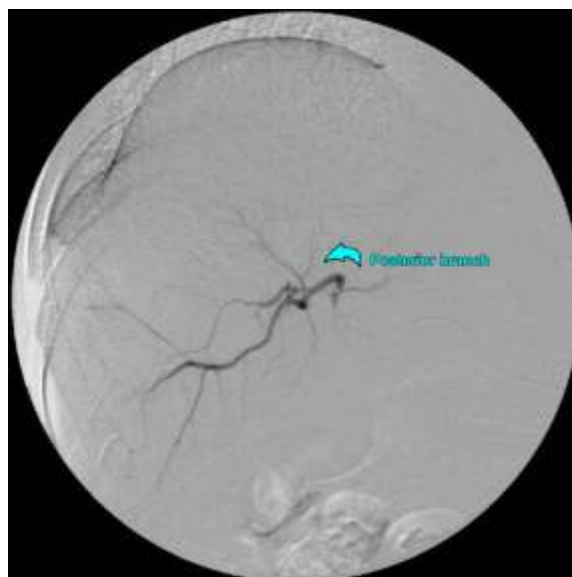
8a.

8b.

8c.

8d.

Figure 8. (a) Celiac arteriography, **(b)** RHA arteriography, and selective arteriography of **(c)** anterior and **(d)** posterior branches in same patient. Images were acquired by using 15° right anterior oblique projections, except for the celiac arteriogram. The anterior branch travels straight right and upward (dark blue arrow). The posterior branch meanders proximally (light blue arrow).

The posterior branch of the RHA divides into inferior (A6) and superior (A7) branches (Fig 9) (27). A6 courses inferolaterally to the lower corner of the liver and it is often the longest and most prominent of the branches that run caudad. A7 is usually identified as a compact complex of meandering vasculature. It appears compact because it runs parallel to the x-ray beam; the tangent of the complex vasculature is evident on projection images.
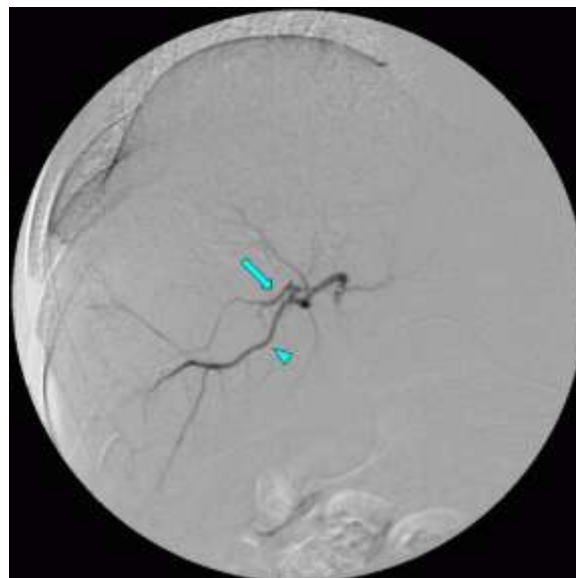
9a.   **9b.**

Figure 9. (a) Celiac arteriography shows posterior branch dividing into A6 and A7. **(b)** Selective arteriography of posterior branch in 15° right anterior oblique projection shows A6 (arrowhead) and A7 (arrow).

A8 and A5 arise from the anterior branch of the RHA (Fig 10). According to the Couinaud classification adopted by Bismuth, the anterior segment of the liver is separated into S8 and S5 (superior and inferior subsegments, respectively) by a transverse plane passing through the right portal vein (14). The bifurcation of the anterior branch is often visualized at arteriography or portography, but territories of the two branches (A8 and A5) after the bifurcation often do not correspond to S8 or S5 of the Couinaud classification adopted by Bismuth (28); instead, both branches course upward (29). Cho et al claimed that the right anterior portal vein does not bifurcate into P8 and P5, but into the right ventral and right dorsal portal veins (30).
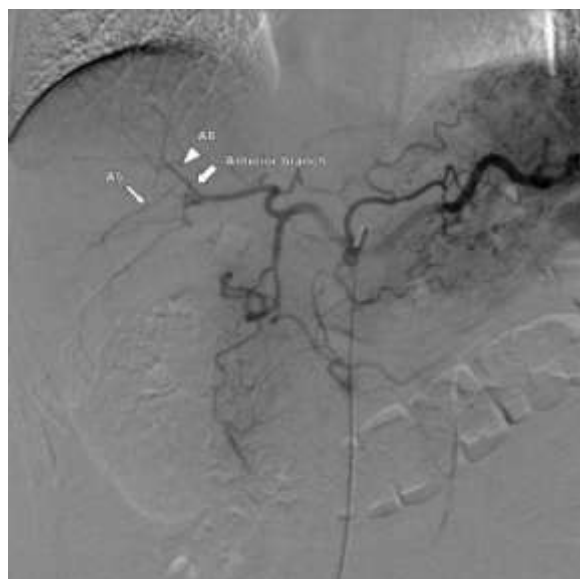

Figure 10. Celiac arteriography shows typical configuration of A5 and A8 branching from the anterior branch.

Since the arterial branches supplying the superior subsegments (S8 and S5) of the anterior segment are called A8, both of the vessels after the bifurcation that course upward can be called A8. In accordance with the notion of Cho et al of a right anterior portal vein bifurcation, it is often practical to call the arterial branches after the bifurcation A8 dorsal and A8 ventral, according to the area that each branch supplies (Fig 11). The A8 dorsal branch usually runs straight up and reaches areas just below the diaphragm. The A8 ventral branch tends to course more ventrally.
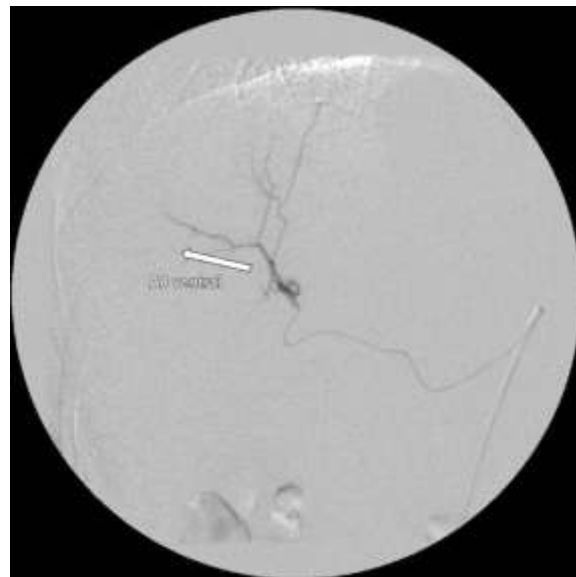

11a.

11b.
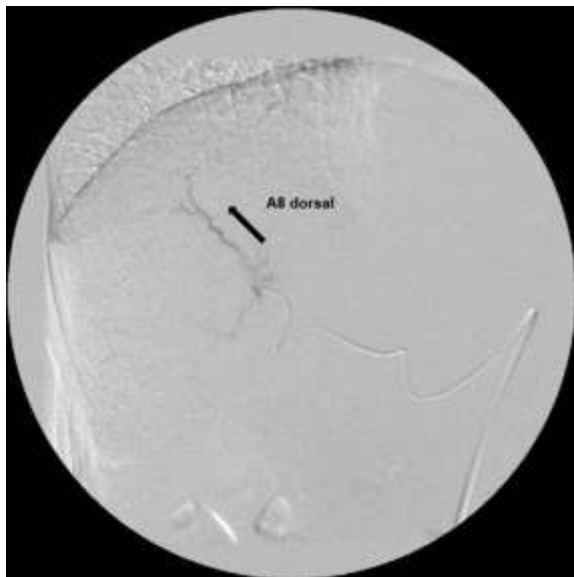
11c.

11d.

Figure 11. (a) Celiac and **(b)** selective arteriography of the anterior branch shows atypical branching that is occasionally seen. After bifurcation of the anterior branch, both branches travel upward and may be referred to as dorsal A8 (black arrow) and ventral A8 (white arrow). Selective arteriography of **(c)** A8 dorsal branch and **(d)** A8 ventral branch.

A5 is usually not a single vessel branching from the anterior branch of the RHA. It represents a group of vessels that branch and course caudad from the anterior branch of the RHA or A8 ventral branch. A5 branches often course downward toward the right but usually appear superior to A6 in the frontal view. The branches are sometimes atrophic and difficult to identify as independent branches at angiography (Fig 12).
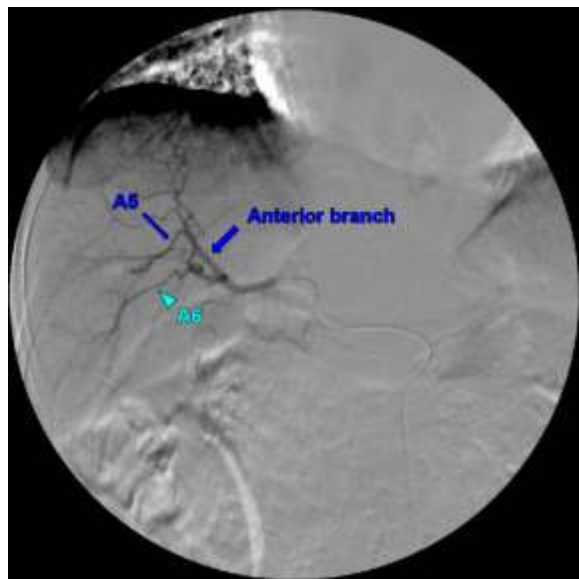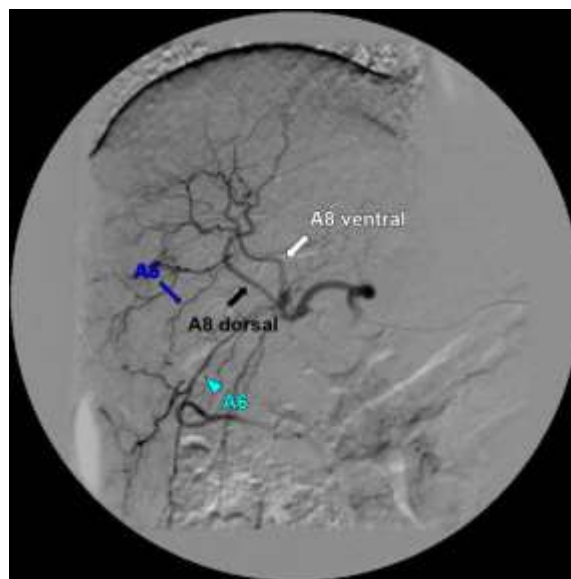

12a.   **12b.**

Figure 12. (a) RHA arteriography in a patient with a prominent A5. The anterior branch and A6 are also seen. **(b)** RHA arteriography in a patient with a dorsal and ventral A8 pattern. A5 arises from the the A8 ventral branch. A8 dorsal branch and A6 are also seen.

Caudate Lobe

The caudate lobe (S1) is supplied by multiple small branches arising from the LHA and RHA (Figs 13, 14) (21,31–32). S1 is supplied by the RHA in only 35% of individuals, by the LHA in 12%, and by both the RHA and LHA in 53% (21). A1 does not designate a single vessel but is a general term for these small arteries. Some of the large branches among them can be identified at angiography. A1 arising from the RHA courses posteriorly and medially and mainly supplies the lateral portion of S1 (the paracaval portion and the papillary process). A1 arising from the LHA courses posteriorly and mainly supplies the medial portion of S1 (caudate process, Spiegel lobe) (32).
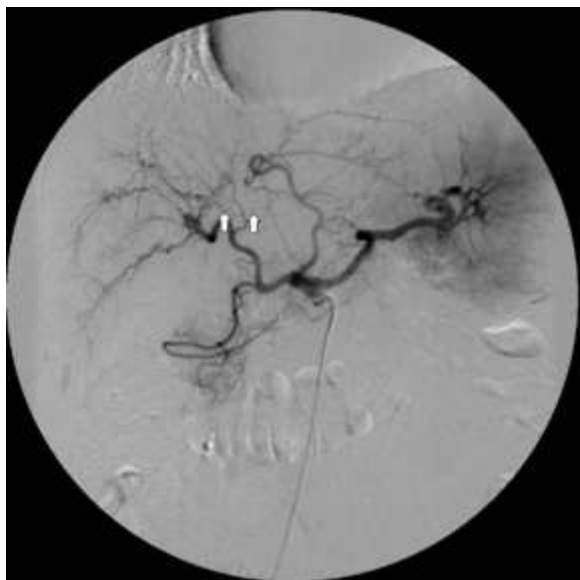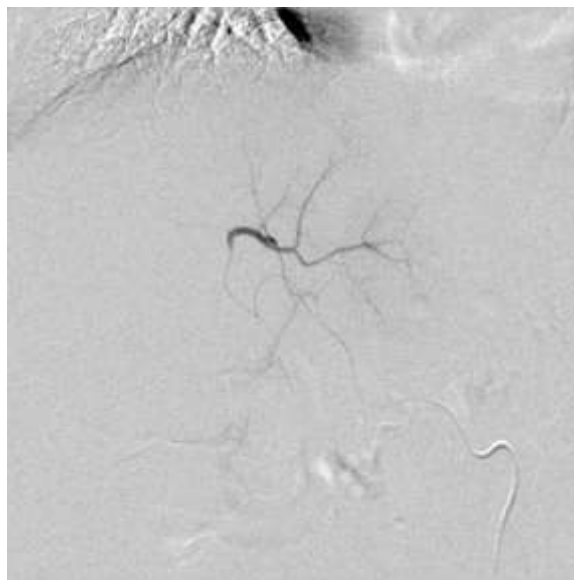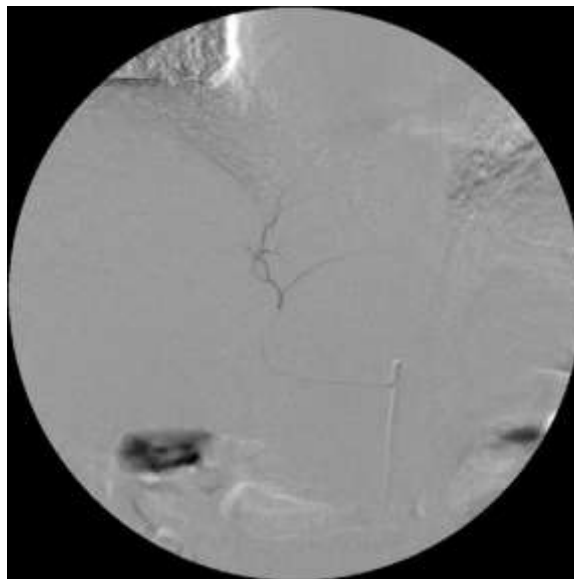
13a.   **13b.**

Figure 13. (a) Celiac arteriography of A1 (arrows) branching from the RHA. **(b)** Selective arteriography of A1 branching from the RHA.

**14a.**   **14b.**

Figure 14. (a) Celiac arteriography of A1 (arrows) branching from the LHA. **(b)** Selective arteriography of A1 branching from the LHA.
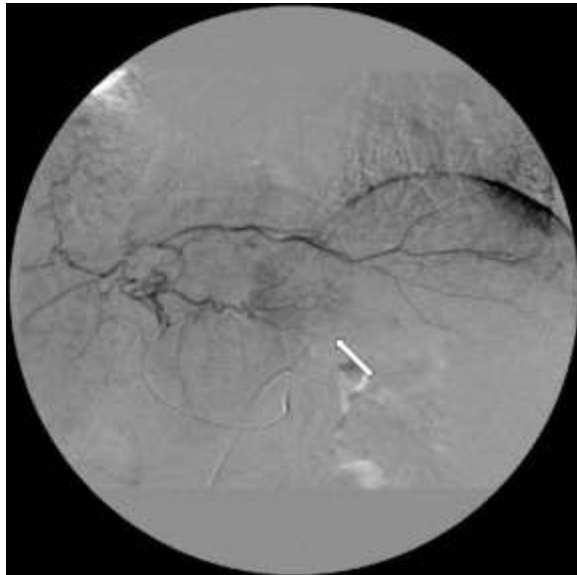
Portal Vein and Branches

Arteriograms and transarterial portograms should be compared to confirm the presence of a portal branch corresponding to each hepatic arterial branch and vice versa (Fig 15). The presence or absence of corresponding vessels suggests mimickers or anatomic variations.

15a.
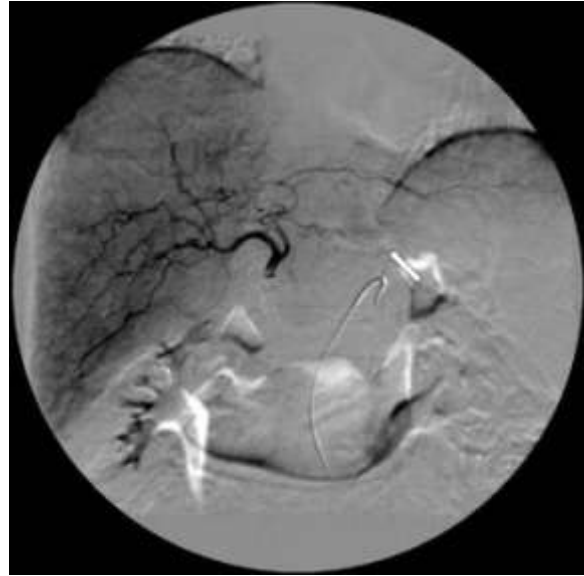
15b.

15c.

Figure 15. (a) Transarterial portography, **(b)** PHA arteriography, and **(c)** LHA arteriography in S3 of same patient after radiofrequency ablation for HCC. Absence of P3 (arrow) indicates P3 occlusion and HCC recurrence, a lesion occupying space, or arterioportal shunting. LHA arteriography clearly reveals HCC recurrence.

The presence of a portal branch without a corresponding artery indicates a replaced or accessory vascular anatomy or transhepatic hepatofugal collateral vessels (33). On the other

hand, the absence of a portal branch corresponding to an arterial branch indicates disease such as portal vein thrombosis, with the arterial branch mimicking the hepatic artery, or arterioportal shunting.

Mimickers of Hepatic Arteries

The arteries supplying adjacent organs of the liver such as the gallbladder and stomach can mimic branches of hepatic arteries.

The cystic artery can mimic RHA branches, especially A6 (Fig 16). The cystic artery is the proximal RHA branch that courses caudad. Bifurcation in the proximal portion, a curved shape that fits that of the gallbladder, and sometimes gallstones can provide clues (27).
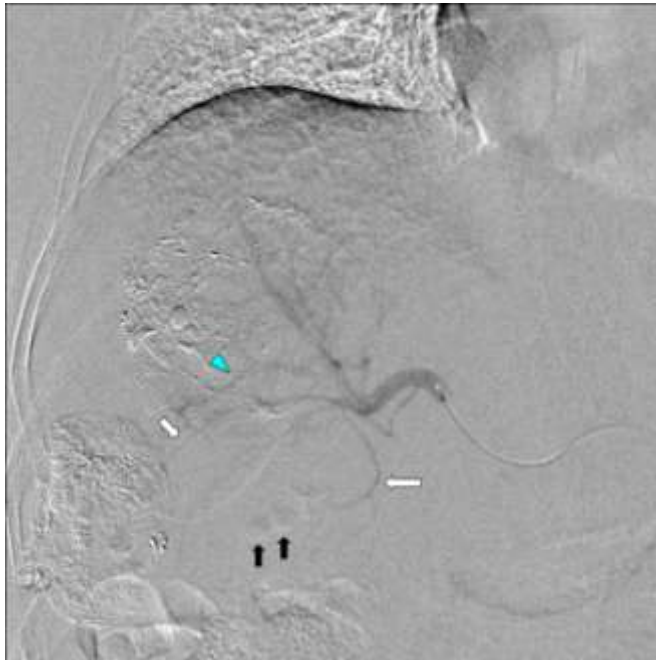

Figure 16. RHA arteriography of cystic artery (white arrows) and A6 (arrowhead). Small gallstones (black arrows) can be seen, and large amounts of lipiodol have been deposited in the right lobe of the liver.

The accessory LGA can mimic A2 or A3 (Fig 17). It branches from the LHA but courses inferior to the umbilical portion of the left portal vein; a gastric bubble and partial enhancement of the gastric mucosa might serve as clues. Enhancement of the gastric mucosa should not be mistaken for a hepatic tumor that requires treatment with embolization.
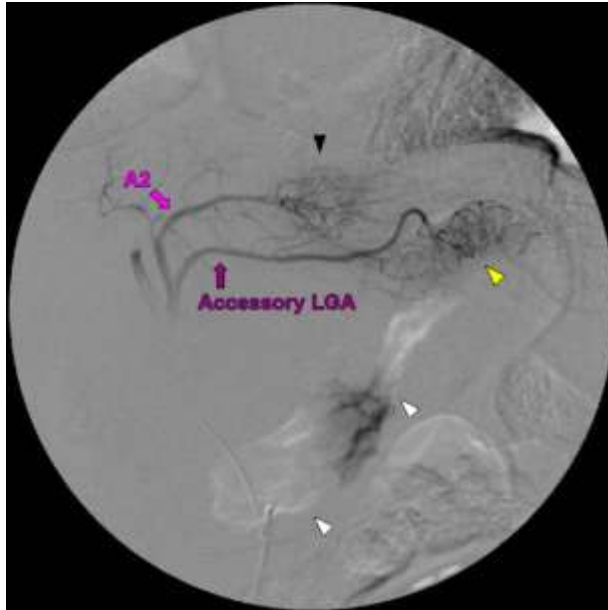
Figure 17. Selective arteriography of accessory LGA shows partially enhanced gastric mucosa (yellow arrowhead). Gastric bubble is also visualized (white arrowheads). Reflux of contrast agent shows A2 and hepatic tumor stain (black arrowhead).

Branches of the LGA can mimic hepatic branches of a replaced LHA (ie, A2, A3, or A4) (Fig 18). The LGA connects to the LHA from the tip of the arch of the LHA when the LHA is replaced (23,25). Therefore, branches after the LHA arch formation are indeed LHA branches (A2, A3, or A4). Comparisons with transarterial portograms might be helpful. Again, partial enhancement of the gastric mucosa and a gastric bubble might serve as clues.
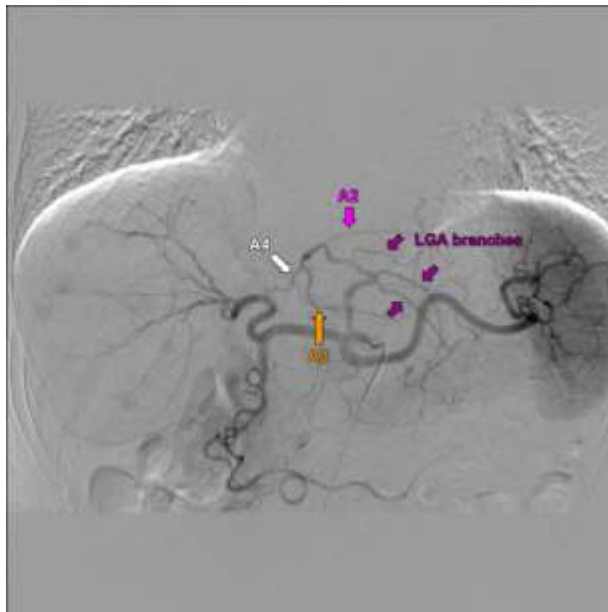

Figure 18. Celiac arteriography of replaced LHA from the LGA. LGA branches mimic hepatic arteries. True hepatic branches of the replaced LHA—A2, A3, and A4—arise after the umbilical portion. Multiple small HCCs are evident in the liver.

The right gastric artery can mimic A3 and sometimes A2 (Fig. 19). It arises from the PHA or LHA, courses inferior to the umbilical portion, and is characterized by distribution to the lesser curvature of the stomach (27).


Figure 19, Movies 1, 2. PHA arteriography of the right gastric artery (white arrows), A2 (pink arrow), and A3 (orange arrow). The right gastric artery courses inferior to the umbilical portion (red arrow). Note that the RHA is replaced in this patient.

Projectional Anatomy of Each Hepatic Segment

The extent of each hepatic segment can be determined at angiography from the territory of the artery supplying the segment. The aim of this section is to define the approximate shape of each segment and how far each segment projects by correlating the course of each segmental branch of the hepatic artery on contrast CT scans during the arterial phase with schematics and celiac and selective arteriography.

The caudate lobe is located behind the hepatic hilum and wraps around the inferior vena cava. The cranial tip of S1 almost reaches the cranial border of the liver. Since A1 usually comprises fine vessels and its frontal side is completely covered by other segments, it is difficult to identify A1 and the S1 border (Fig 20, Movies 1, 2).
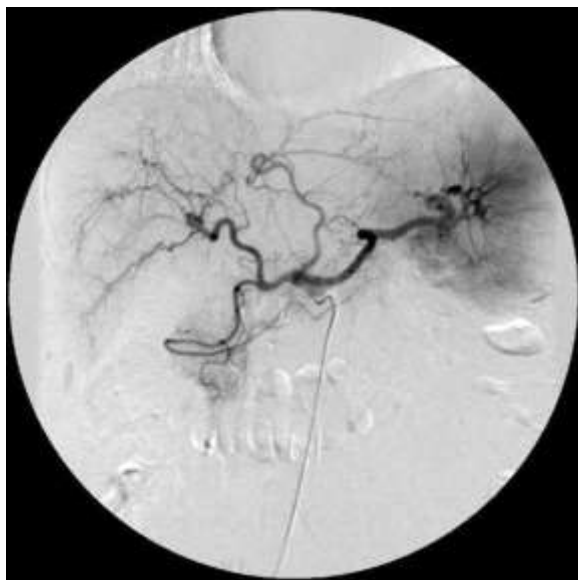
20a. **20b.**

Figure 20. (a) Celiac arteriography and **(b)** drawing show location of S1 in liver.

S2 delineates the diaphragmatic surface of the anatomic left lobe and occupies the left corner of the liver. The lower border of S2 is usually positioned craniad to the inferior border of the left lobe. S2 is bordered by the umbilical portion on the right side and is located dorsally on the transaxial plane. It is often horizontally elongated in cirrhosis (Fig 21, Movies 3, 4).
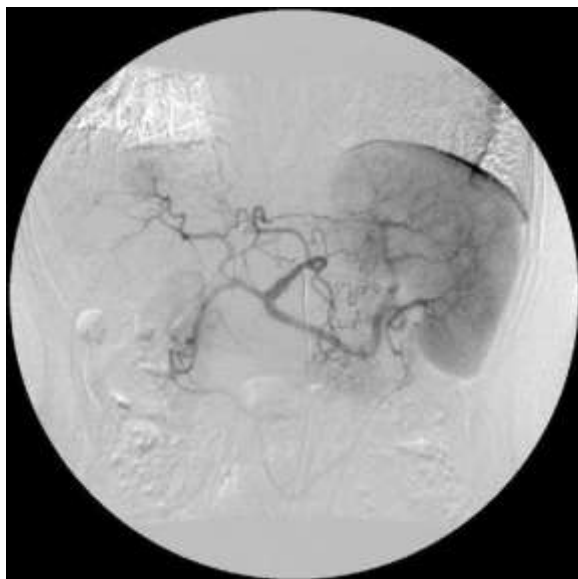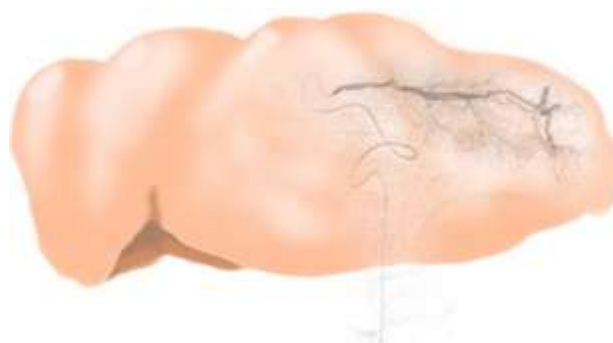
21a. **21b.**

Figure 21, Movies 3,4. (a) Celiac arteriography and **(b)** drawing show location of S2 in liver.

S3 occupies the caudal portion of the anatomic left lobe and delineates the inferior border of the left lobe. The areas occupied by S2 and S3 overlap in the frontal view because the border between them leans. S3 is bordered by the umbilical portion on the right side. In the transaxial plane, it becomes thinner in the caudal portion, where it is located along the frontal abdominal

wall, covering the stomach and pancreas. An accessory LGA, right gastric artery, and replaced LHA from the LGA can mimic A3 (Fig 22, Movies 5, 6).


22a.   **22b.**

Figure 22, Movies 5,6. (a) Celiac arteriography and **(b)** drawing show location of S3 in liver.

The cranial border of S4 coincides with that of the liver. The caudal border of S4 also comes close to that of the liver but is often superimposed by S6 on projection images. S4 is bordered by the umbilical portion of the left portal vein on the left, and its right border almost reaches the center of the right lobe. S4 is often atrophic in viral cirrhosis. It covers the frontal surfaces of the hepatic hilum, S1, and the medial portion of the posterior segment (Fig 23, Movies 7, 8).
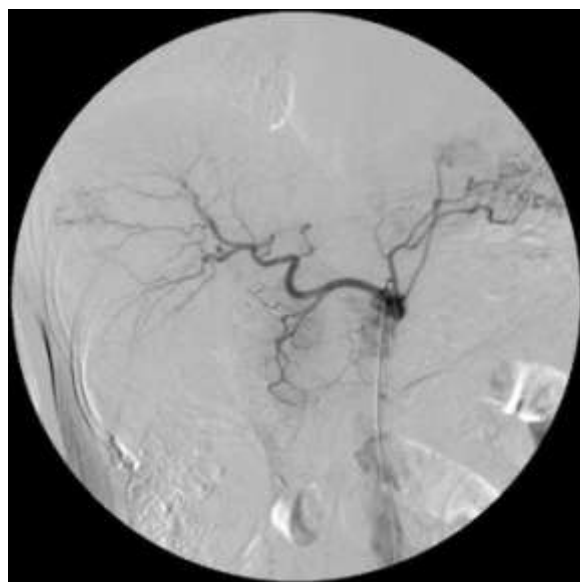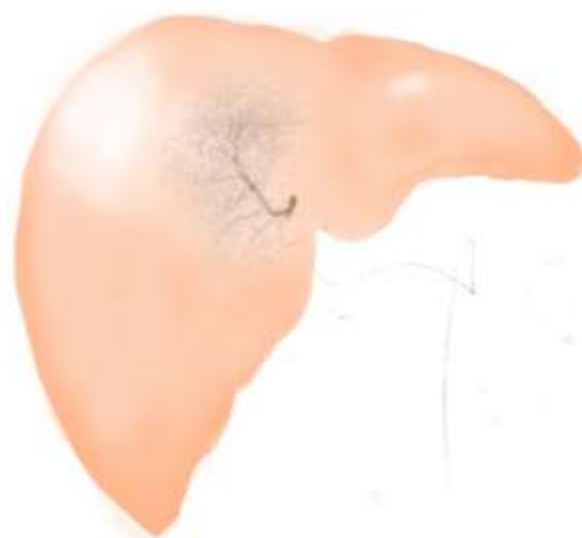
23a.   **23b.**
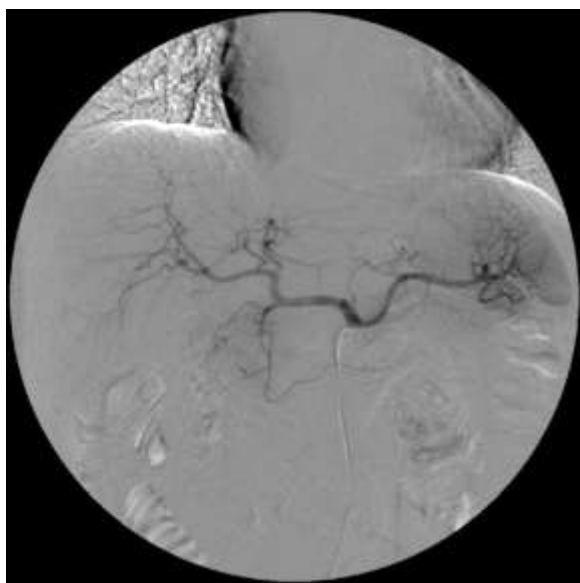
Figure 23, Movies 7,8. (a) Celiac arteriography and **(b)** drawing show location of S4 in liver.

S5 has a quadrilateral shape, delineating the right border of the right lobe. Although S5 occupies the lower portion of the right border of the right lobe, the inferior corner is occupied by S6 (Fig 24, Movies 9, 10).
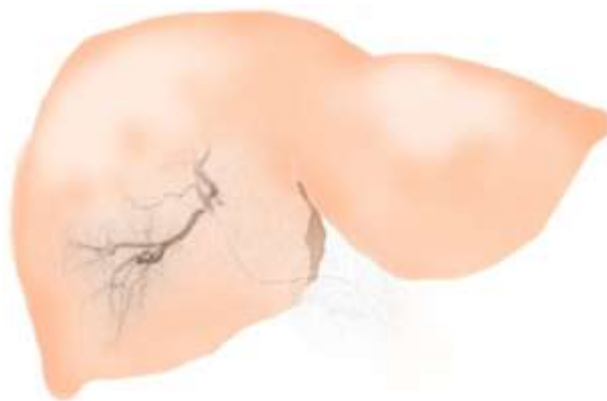
24a.   24b.

Figure 24, Movies 9,10. (a) Celiac arteriography and **(b)** drawing show location of S5 in liver.

S6 appears as a parallelogram delineating the caudal end of the right border and occupies the inferior corner of the liver. It also delineates the inferior border of the right lobe (Fig 25, Movies 11, 12).
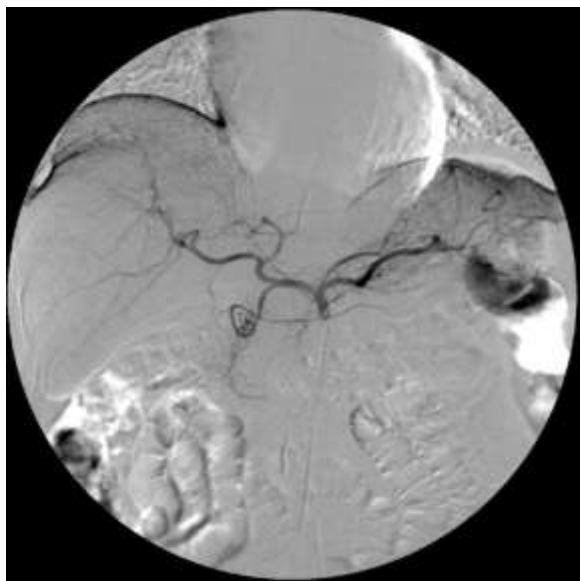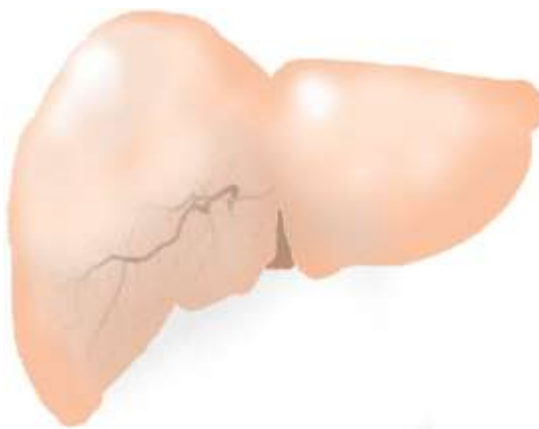
25a.   25b.

Figure 25, Movies 11-13. (a) Celiac arteriography and **(b)** drawing show locations of S6 and S7 in liver.

S7 occupies the central portion of the right lobe in the frontal view. Since the frontal border of S7 is completely covered by S4, S8, S5, and S6, it does not delineate any border of the liver (Fig 25, Movies 11, 13).

S8 appears as an inverted triangle, with the base being the diaphragm, and occupies a wide area below the diaphragmatic dome. It also delineates the cranial portion of the right border of the right lobe (Fig 26, Movies 14, 15).
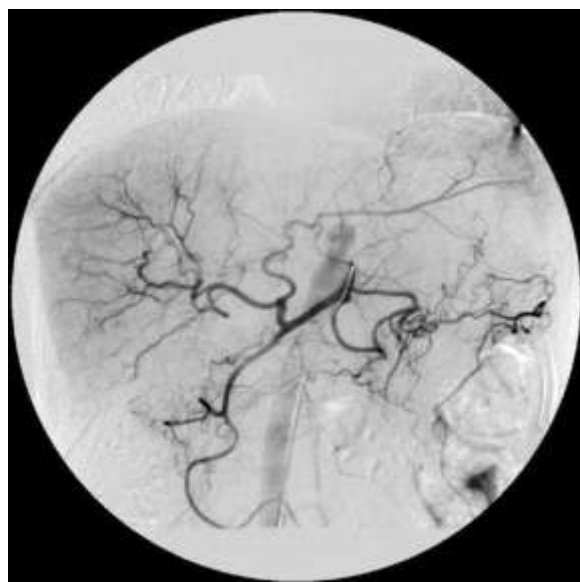

26a.   26b.

Figure 26, Movies 14, 15. (a) Celiac arteriography and **(b)** drawing show location of S8 in liver.

Changes with the Respiratory Cycle

The liver moves and deforms during the respiratory cycle. Besides the craniocaudal movement that is the dominant component of the motion, anteroposterior and lateral movements and deformations are not negligible (34). At tidal inspiration, the liver moves about 10–26 mm downward and about 1 cm in the anteroposterior and lateral directions (34–36). The reported amount of liver rotation is less than 1.5° but the precise amount remains obscure (36).

Respiratory motion usually has more adverse than favorable effects on interventional angiography. The most common adverse effect is imperfect breath-holding during digital subtraction angiography, resulting in artifacts and decreased image quality. However, since the dominant direction of respiratory movement is craniocaudal, the adverse effects of imperfect breath-holding can usually be compensated for by translating the masking image upward or downward.

Respiratory motion can also prevent insertion of a catheter or guidewire into the intended vessel; a guidewire might also dissociate from a selected vessel during a cough. Respiratory motion can sometimes help guidewire manipulation; when selecting an artery is troublesome, the patient should be asked to breathe deeply or cough.

Little is known about the respiratory deformation of hepatic vessels or the liver itself. We therefore created a virtual movie to demonstrate deviation and distortion of the intrahepatic portal veins and arteries (Fig 27, Movie 16). The movie was created from dynamic CT data in which the arterial and venous phases were acquired at end expiration and deep inspiration, respectively. We manually placed 200 pairs of landmark points on both images and then

calculated the respiratory translation of all of the points by using radial basis function–based interpolation (37,38) to reconstruct the virtual movie.
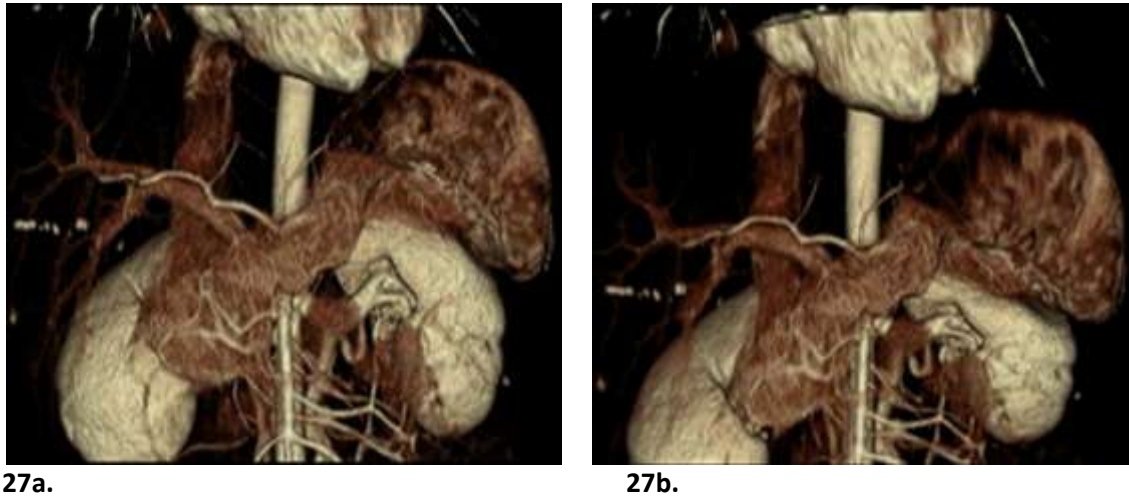
27a.   **27b.**

Figure 27, <u>Movie 16</u>. Frames from Movie 16 during **(a)** expiratory and **(b)** inspiratory phases.

Conclusions

Each segmental branch of the hepatic artery and mimickers can be distinguished by the morphologic characteristics of each vessel. The location of each hepatic segment on angiograms can be estimated if the artery supplying the segment can be correctly identified. Recognizing morphologic differences in the hepatic artery system caused by respiration is important.

References

1. Gomaa AI, Khan SA, Toledano MB, Waked I, Taylor-Robinson SD. Hepatocellular carcinoma: epidemiology, risk factors and pathogenesis. World J Gastroenterol 2008;14(27): 4300-4308.
2. Mazzanti R, Gramantieri L, Bolondi L. Hepatocellular carcinoma: epidemiology and clinical aspects. Mol Aspects Med 2008;29(1,2):130-143.
3. Lau WY, Lai EC. Hepatocellular carcinoma: current management and recent advances. Hepatobiliary Pancreat Dis Int 2008;7(3):237-257.
4. Seeff LB, Hoofnagle JH. Epidemiology of hepatocellular carcinoma in areas of low hepatitis B and hepatitis C endemicity. Oncogene 2006;25(27):3771-3777.
5. Di Bisceglie AM. Epidemiology and clinical presentation of hepatocellular carcinoma. J Vasc Interv Radiol 2002;13(9,Pt 2):S169-S171.
6. Matsui O, Kadoya M, Kameyama T, et al. Benign and malignant nodules in cirrhotic livers: distinction based on blood supply. Radiology 1991;178(2):493-497.
7. Takayasu K, Muramatsu Y, Furukawa H, et al. Early hepatocellular carcinoma: appearance at CT during arterial portography and CT arteriography with pathologic correlation. Radiology 1995;194(1):101-105.
8. Kim HC, Kim TK, Sung KB, et al. CT during hepatic arteriography and portography: an illustrative review. Radiographics 2002;22(5):1041-1051.
9. Ibrahim SM, Lewandowski RJ, Sato KT, et al. Radioembolization for the treatment of unresectable hepatocellular carcinoma: a clinical review. World J Gastroenterol 2008;14(11):1664-1669.

10. Hjortsjö CH. The topography of the intrahepatic duct systems. Acta Anat 1951;11(4):599-615.
11. Healey JE Jr, Schroy PC. Anatomy of the biliary ducts within the human liver: analysis of the prevailing pattern of branchings and the major variations of the biliary ducts. AMA Arch Surg 1953;66(5):599-616.
12. Couinaud C. Le foie: etudes anatomiques et chirurgicales. Paris: Masson, 1957.
13. Goldsmith NA, Woodburne RT. The surgical anatomy pertaining to liver resection. Surg Gynecol Obstet 1957;105(3):310-318.
14. Bismuth H. Surgical anatomy and anatomical surgery of the liver. World J Surg 1982;6(1):3-9.
15. Federative Committee on Anatomical Terminology. Terminologia anatomica: international anatomical terminology. Stuttgart, Germany: Thieme, 1998;54-56.
16. Brancatelli G, Federle MP, Ambrosini R, et al. Cirrhosis: CT and MR imaging evaluation. Eur J Radiol 2007;61(1):57-69.
17. Lunderquist A. Arterial segmental supply of the liver: an angiographic study. Acta Radiol Diagn (Stockh) 1967:Suppl 272:1-81.
18. Bierman HR, Byron RL Jr, Kelley KH, Grady A. Studies on the blood supply of tumors in man. III. Vascular patterns of the liver by hepatic arteriography in vivo. J Natl Cancer Inst 1951;12(1):107-131.
19. Ruzicka FF Jr, Rossi P. Normal vascular anatomy of the abdominal viscera. Radiol Clin North Am 1970;8(1):3-29.
20. Michels NA. Variational anatomy of the hepatic, cystic, and retroduodenal arteries: a statistical analysis of their origin, distribution, and relations to the biliary ducts in two hundred bodies. AMA Arch Surg 1953;66(1):20-34.
21. Michels NA. Blood supply and anatomy of the upper abdominal organs with a descriptive atlas. Philadelphia, Pa: Lippincott, 1955.
22. Stulberg JH, Bierman HR. Selective hepatic arteriography: normal anatomy, anatomic variations, and pathological conditions. Radiology 1965;85:46-55.
23. Gruttadauria S, Foglieni CS, Doria C, Luca A, Lauro A, Marino IR. The hepatic artery in liver transplantation and surgery: vascular anomalies in 701 cases. Clin Transplant 2001;15(5):359-363.
24. Liu DM, Salem R, Bui JT, et al. Angiographic considerations in patients undergoing liver-directed therapy. J Vasc Interv Radiol 2005;16(7):911-935.
25. Kusano S, Matsubayashi T, Ishii K. The evaluation of the angiographic "umbilical point" of the left hepatic artery. Nippon Igaku Hoshasen Gakkai Zasshi 1976;36(1):7-12.
26. Hiramatsu K, Kouda E, Mouri M, Isobe Y. X-ray anatomy of the abdominal vascular system. Tokyo, Japan: Igaku-Shoin, 1982;63-82.
27. Kadir S, Lundell C, Saeed M. Celiac, superior, and inferior mesenteric arteries. In: Kadir S, ed. Atlas of normal and variant angiographic anatomy. Philadelphia, Pa: Saunders, 1991;297-364.
28. Cho A, Okazumi S, Takayama W, et al. Anatomy of the right anterosuperior area (segment 8) of the liver: evaluation with helical CT during arterial portography. Radiology 2000;214(2):491-495.
29. Kogure K, Kuwano H, Fujimaki N, Ishikawa H, Takada K. Reproposal for Hjortsjo's segmental anatomy on the anterior segment in human liver. Arch Surg 2002;137(10):1118-1124.

30. Cho A, Okazumi S, Miyazawa Y, et al. Proposal for a reclassification of liver based anatomy on portal ramifications. Am J Surg 2005;189(2):195-199.
31. Miyayama S, Matsui O, Kameyama T, et al. Angiographic anatomy of arterial branches to the caudate lobe of the liver with special reference to its effect on transarterial embolization of hepatocellular carcinoma. Rinsho Hoshasen 1990;35(3):353-359.
32. Yoon CJ, Chung JW, Cho BH, et al. Hepatocellular carcinoma in the caudate lobe of the liver: angiographic analysis of tumor-feeding arteries according to subsegmental location. J Vasc Interv Radiol 2008;19(11):1543-1550.
33. Bron K, Baum R. Arterial portography. In: Baum S, ed. Abrams angiography, vascular and interventional radiology, 4th ed. Boston, Mass: Little, Brown, 1997;1527-1548.
34. Clifford MA, Banovac F, Levy E, Cleary K. Assessment of hepatic motion secondary to respiration for computer assisted interventions. Comput Aided Surg 2002;7(5):291-299.
35. Shimizu S, Shirato H, Xo B, et al. Three-dimensional movement of a liver tumor detected by high-speed magnetic resonance imaging. Radiother Oncol 1999;50(3):367-370.
36. Rohlfing T, Maurer CR Jr, O'Dell WG, Zhong J. Modeling liver motion and deformation during the respiratory cycle using intensity-based nonrigid registration of gated MR images. Med Phys 2004;31(3):427-432.
37. Arad N, Reisfeld D. Image warping using few anchor points and radial functions. Comput Graphics Forum 1995;14(1):35-46.
38. Fornefett M, Rohr K, Stiehl HS. Radial basis functions with compact support for elastic registration of medical images. Image Vision Comput 2001;19(1,2):87-96.

RadioGraphics *(vertical side text)*

Hepatic Segments and Vasculature: Projecting CT Anatomy onto Angiograms

Toshihiro Furuta, MD, *et al*

Teaching Point 1
Radiologists should understand the anatomy of the hepatic vasculature and confirm on conventional angiograms the location of an artery or lesion seen at CT.

Teaching Point 2
At the posterior (dorsal) part of the umbilical portion of the left portal vein, the LHA overrides the portal vein to form the arch of the LHA. This arch is characteristic of the LHA and is helpful in distinguishing it from mimickers.

Teaching Point 3
The RHA divides into anterior and posterior branches that are characterized by a straight right upward course and by a meandering proximal portion, respectively (Fig 8).

Teaching Point 4
The presence of a portal branch without a corresponding artery indicates a replaced or accessory vascular anatomy or transhepatic hepatofugal collateral vessels.

Teaching Point 5
The absence of a portal branch corresponding to an arterial branch indicates disease such as portal vein thrombosis, with the arterial branch mimicking the hepatic artery, or arterioportal shunting.